JB
Journals.ASM.org

Defining the *Escherichia coli* SecA Dimer Interface Residues through *In Vivo* Site-Specific Photo-Cross-Linking

Dongmei Yu,[a] Andy J. Wowor,[a]* James L. Cole,[b,c] Debra A. Kendall[a]

Department of Pharmaceutical Sciences,[a] Department of Molecular and Cell Biology,[b] and Department of Chemistry,[c] University of Connecticut, Storrs, Connecticut, USA

The motor protein SecA is a core component of the bacterial general secretory (Sec) pathway and is essential for cell viability. Despite evidence showing that SecA exists in a dynamic monomer-dimer equilibrium favoring the dimeric form in solution and in the cytoplasm, there is considerable debate as to the quaternary structural organization of the SecA dimer. Here, a site-directed photo-cross-linking technique was utilized to identify residues on the *Escherichia coli* SecA (*ec*SecA) dimer interface in the cytosol of intact cells. The feasibility of this method was demonstrated with residue Leu6, which is essential for *ec*SecA dimerization based on our analytical ultracentrifugation studies of SecA L6A and shown to form the cross-linked SecA dimer *in vivo* with *p*-benzoyl-phenylalanine (*p*Bpa) substituted at position 6. Subsequently, the amino terminus (residues 2 to 11) in the nucleotide binding domain (NBD), Phe263 in the preprotein binding domain (PBD), and Tyr794 and Arg805 in the intramolecular regulator of the ATPase 1 domain (IRA1) were identified to be involved in *ec*SecA dimerization. Furthermore, the incorporation of *p*Bpa at position 805 did not form a cross-linked dimer in the SecA Δ2-11 context, indicating the possibility that the amino terminus may directly contact Arg805 or that the deletion of residues 2 to 11 alters the topology of the naturally occurring *ec*SecA dimer.

The majority of bacterial secretory proteins are posttranslationally translocated across the cytoplasmic membrane by the evolutionarily conserved general secretory (Sec) system (for a review, see reference 1), in which SecA receives unfolded newly synthesized preproteins from the molecular chaperone SecB (2) and inserts them into the membrane-embedded heterotrimeric SecYEG channel in an ATP-dependent manner (3). Structural studies of the key components of this system, including the SecA translocation motor, and dynamic analyses of their interactions are critical to understanding the Sec-dependent protein translocation process.

In *Escherichia coli*, SecA is a 901-amino-acid multidomain protein (102 kDa) containing the ATPase DEAD box motor consisting of two domains (nucleotide binding domain [NBD] and intramolecular regulator of ATPase 2 [IRA2]), the preprotein binding domain (PBD), the helical scaffold domain (SD), IRA1, the helical wing domain (WD), and the carboxy-terminal domain (CTD) (4). The large, multidomain structure and the cytosolic and inner membrane localization of SecA (5) reflect its multiple functions, including interaction with nucleotides, SecB, preproteins, and membrane phospholipids (6) and SecYEG (7). In solution, the SecA homodimer was examined by size exclusion chromatography, sucrose gradient ultracentrifugation, and chemical cross-linking (8), and the monomer-dimer equilibrium was shown to be affected not only by environmental factors such as salt concentration and temperature (9, 10) but also by translocation ligands such as ATP (11, 12), phospholipid (13, 14), and signal peptides (10, 12–15). At physiological salt concentration (ionic strength [I] = 150 mM), SecA exists in a reversible monomer-dimer equilibrium with a dissociation constant (K_d) below 0.3 μM (9, 10), which is substantially lower than the estimated intracellular SecA concentration of ~2.5 μM (13). Therefore, *in vivo* cytosolic SecA likely exists in a monomer-dimer equilibrium favoring the dimeric form. During the translocation process, a SecA dimer is thought to bind SecB (16); however, the functional oligomeric state of SecA for SecYEG binding remains controversial (17–22).

The five crystal structures described to date for dimeric SecA (4, 23–26) all exhibit distinctly different dimer interfaces, although protomers from different bacterial species share a conserved structure. With the exception of the WD and CTD, each domain is involved in intersubunit contacts of dimeric SecA in at least one crystal structure. Although the DEAD box motor is located on the interface of each SecA dimer structure, the proposed interfacial residues vary. Interestingly, the extreme amino terminus comprises the intersubunit interface of both the antiparallel *Bacillus subtilis* SecA (*bs*SecA) dimer (23, 27) and the parallel *Thermus thermophilus* SecA (*tt*SecA) dimer (26).

Various approaches have been used to locate residues on the SecA dimer interface. Deletion of residues 2 to 11 was shown to promote *E. coli* SecA (*ec*SecA) monomers using chemical cross-linking, size exclusion chromatography, and sucrose gradient centrifugation (17, 28), suggesting that those residues are essential for *ec*SecA dimerization; however, deletion of residues 2 to 8 had a more subtle impact on *ec*SecA oligomerization, resulting in a K_d only 10-fold higher than that of wild-type *ec*SecA as determined by size exclusion chromatography (29). Intermolecular interaction via Arg750 and Gly587 of *bs*SecA or their counterparts of *ec*SecA was suggested by disulfide cross-linking (17, 19, 25). In addition, based on sequence similarity, one study employed a SecA/N95 mutant containing six alanine substitutions

Received 26 December 2012 Accepted 5 April 2013
Published ahead of print 12 April 2013
Address correspondence to Debra A. Kendall, debra.kendall@uconn.edu.
* Present address: Andy J. Wowor, Department of Chemistry and Biochemistry, Colorado College, Colorado Springs, Colorado, USA.
Supplemental material for this article may be found at http://dx.doi.org/10.1128/JB.02269-12.

doi:10.1128/JB.02269-12

in the IRA1 domain (F808A M810A F811A M814A L815A L818A) and showed that the mutant protein sedimented at a position slightly faster than that of bovine serum albumin (BSA) (67 kDa), indicating that this region is important for SecA dimerization (13). However, it remains unclear which specific residues are on the dimer interface.

Recently, a site-directed *in vivo* photo-cross-linking method (30) was successfully utilized to investigate interfacial residues in protein-protein complexes (31–33), including SecA-SecY (34, 35) and SecA-SecG (35). In this experimental system, the photoreactive amino acid analog *p*-benzoyl-phenylalanine (*p*Bpa) is incorporated into nascent polypeptide chains at amber mutation (TAG) sites. Upon irradiation of intact cells, *p*Bpa reacts covalently with carbon-hydrogen bonds within 3 Å (36). Thus, this provides a method for *in vivo* cross-linking of interacting partners in cells and identification of residues on the interface of oligomers. Here, this site-specific *in vivo* cross-linking method was utilized to identify residues on the *ec*SecA dimer interface. Our results demonstrate that the extreme amino terminus participates in SecA dimerization, consistent with the monomerization of SecA Δ2-11 shown by analytical ultracentrifugation (AUC). Residues Phe263 in the PBD and Tyr794 and Arg805 in the IRA1 domain are also involved in SecA dimerization. Interestingly, our data indicate that removal of residues 2 to 11 in SecA impacts the *in vivo* cross-linking profile and that residue Arg805 cross-linking is strongly diminished in SecA Δ2-11.

MATERIALS AND METHODS

Plasmids. The *secA* gene fused to a carboxy-terminal His tag on a modified ampicillin-resistant vector pET-29b (37) results in the plasmid pET29b-SecA-His. SecA variants in this study, including those with deletions and substitutions, were generated with the QuikChange site-directed mutagenesis system (Agilent Technologies) and confirmed by DNA sequencing. The plasmid pEVOL-uaaRS, used for the efficient incorporation of *p*Bpa at amber stop codons (TAG) (38), was kindly provided by P.G. Schultz (The Scripps Research Institute). Following the nomenclature used by Schultz and colleagues (38), in this paper, X was used to denote substitution of the unnatural amino acid *p*Bpa. To facilitate the detection of dimeric SecA, a second SecA-expressing plasmid, pCDF-SecA-myc, was obtained by subcloning *secA* with a c-myc tag on the carboxy terminus into the NcoI/XhoI-digested pCDF-1b plasmid (Novagen). The plasmid pCDF-1b, which possesses the CloDF13 origin of replication and confers streptomycin resistance, is compatible with the pET-29b (ColE1 origin and ampicillin resistance) and pEVOL-uaaRS (P15A origin and chloramphenicol resistance) plasmids, thus making coexpression of SecA and its amber mutant proteins possible.

Protein expression, purification, and AUC. All proteins were expressed in *E. coli* strain BL21(DE3). Protein samples of SecA-His and its amino-terminal deletion and substitution variants were purified with an Ni-nitrilotriacetic acid (NTA) agarose column (Qiagen) and further purified following a previously described protocol (10). The protein concentration was determined by absorption at 280 nm using an extinction coefficient calculated with the program Sednterp (39).

Sedimentation experiments were carried out with an Optima XL-I analytical ultracentrifuge (Beckman Coulter). For sedimentation velocity measurements, samples (420 μl, concentrations of 0.5, 1, 5, and 10 μM) and reference solution (430 μl) were loaded into cells and centrifuged at 40,000 rpm using an An-50 Ti rotor at 20°C. Interference scans were collected at intervals of 1 min for 6 h. Multiple data sets were fit to a monomer-dimer equilibrium plus incompetent species model (10) with the software SEDANAL (40) to obtain the dissociation constants.

***In vivo* photo-cross-linking, protein preparation, and Western blot evaluation.** To express *p*Bpa-substituted SecA, pEVOL-uaaRS and a SecA amber mutant plasmid were cotransformed into BL21(DE3) cells. Coexpression of SecA containing no *p*Bpa was performed by simultaneously transforming plasmid pCDF-SecA-myc. Cells were cultured in 50 ml LB medium with appropriate antibiotics. The working antibiotic concentrations were as follows: ampicillin, 100 μg/ml; chloramphenicol, 50 μg/ml; and streptomycin, 50 μg/ml. Production of proteins was induced by the addition of 0.2 μM *p*Bpa (Bachem), 0.02% L-arabinose, and 1 mM IPTG (isopropyl-β-D-thiogalactopyranoside) at an optical density at 600 nm (OD_{600}) of ~0.6. After growing for another 1.5 to 2 h, the induced cells were harvested by centrifugation, washed in a half volume of phosphate-buffered saline (PBS) (10 mM NaH_2PO_4 [pH 7.2], 140 mM NaCl), and then stored at −80°C.

For photo-cross-linking experiments, cells were resuspended in PBS to an OD_{600} of ~0.8. A 6-ml volume of cells was transferred to a polystyrene petri dish (3.5-cm diameter) on ice and irradiated with a Spectroline Built-in-Ballast UV lamp (model BIB-150P, 365 nm) for 15 min. Irradiated cells were lysed with 200 μl of Bugbuster protein extraction reagent (Novagen) supplemented with 1 mg/ml lysozyme, 50 μg/ml DNase I, and 0.5 mM phenylmethylsulfonyl fluoride (PMSF). The soluble fraction was used for Western blot analysis.

Comparable amounts of protein were resolved on 7.5% SDS-polyacrylamide gels and electroblotted onto polyvinylidene difluoride (PVDF) membranes (Millipore). Nonspecific binding was blocked with 5% nonfat milk (Bio-Rad) in PBS-T (100 mM NaH_2PO_4 [pH 7.5], 100 mM NaCl, and 0.05% Tween 20). The membrane was incubated with either the monoclonal mouse anti-His (GenScript) or the anti-c-myc (Calbiochem) antibody and detected with a horseradish peroxidase (HRP)-conjugated goat anti-mouse antibody (GenScript). The signal was developed by addition of the SuperSignal West Femto chemiluminescent substrate (Thermo Scientific) and visualized on X-ray film.

Protein identification by mass spectroscopy. Cells expressing a *p*Bpa-containing SecA amber mutant were collected from a 500-ml culture by centrifugation. The PBS washing, UV-cross-linking, and cell lysis steps were as described above. The supernatant was applied to an Ni-NTA column (Qiagen), and the SecA mutant protein and any cross-linked product were eluted. The protein sample was separated on a 7.5% SDS-polyacrylamide gel, followed by an in-gel tryptic digestion (41) of the band of interest. Protein identification by liquid chromatography-electrospray ionization coupled to tandem mass spectrometry (LC-ESI-MS/MS) was performed at the UAlbany Proteomics Facility (Rensselaer, NY) as follows. The extracted peptides were separated by high-performance liquid chromatography (CapLC; Waters) on a Vydac Everest C_{18} column interfaced to an electrospray time-of-flight tandem mass spectrometer (QSTAR XL; AB Sciex). Tandem mass spectra were compared with the NCBI nonredundant *E. coli* database using the Mascot algorithm (Matrix-Science) to identify the cross-linked partner of SecA.

Dimeric interface analysis. All SecA structures used in this study are from the RCSB Protein Data Bank (http://www.rcsb.org), except for a *bs*SecA dimer (Div_dimer) (23, 27) kindly provided by J. F. Hunt (Columbia University). The dimeric interface residues were predicted with the SPPIDER (solvent accessibility-based protein-protein interface identification and recognition) algorithm (42), based on the relative solvent accessibilities of amino acid residues.

RESULTS

AUC sedimentation velocity analysis of SecA amino-terminal variants. First, we used AUC to establish that the His tag fused to the carboxy terminus of SecA does not alter its monomer-dimer equilibrium. Previously, we have applied sedimentation velocity to determine SecA monomer-dimer dissociation constants under various conditions (10). Figure 1A shows an overlay of normalized g(s*) sedimentation coefficient distributions obtained at multiple SecA-His concentrations in 300 mM KCl buffer. The peak of the

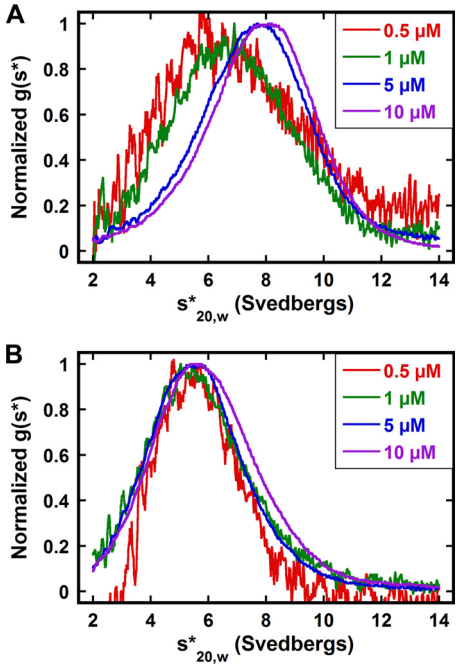

FIG 1 Sedimentation velocity analysis of SecA (A) and SecA Δ2-11 (B) in 300 mM KCl buffer, shown as normalized g(s*) distributions. Each distribution represents a different protein concentration. The distributions are normalized by amplitude. The sedimentation velocity measurements were performed as described in Materials and Methods.

distribution moves to the right as the protein concentration increases from 0.5 μM to 10 μM (Fig. 1A), revealing reversible association. Global analysis of these data indicates that the K_d of SecA-His is 3.65 ± 0.19 μM (Table 1) and is comparable to that of untagged SecA (10), indicating that there is no significant effect of the carboxy-terminal His tag on the association properties of SecA. Consequently, the pET29b-SecA-His plasmid was used to generate SecA variants, and here, wild-type SecA refers to SecA with the carboxy-terminal His tag.

Second, we characterized the association of SecA Δ2-11. In contrast to the case for wild-type SecA, the g(s*) distributions for SecA Δ2-11 do not shift with increasing concentration from 0.5 μM to 10 μM (Fig. 1B). The distribution peak at a sedimentation coefficient of ~5.6 S corresponds to the SecA monomer, indicating that SecA Δ2-11 does not associate in 300 mM KCl buffer. This is consistent with the largely monomeric form of SecA Δ2-11/N95 observed using sucrose gradient centrifugation and size exclusion chromatography (17, 28). However, like for SecA without a His tag (10), lower salt concentrations promote the self-association of SecA Δ2-11. In 100 and 200 mM KCl buffers, the sedimentation coefficient distribution shifts to the right with increasing SecA Δ2-11 concentration, indicating reversible dimerization. When the salt concentration changes from 200 mM to 100 mM, the K_d of SecA Δ2-11 decreases ~200-fold from 29.87 μM to 0.13 μM, whereas the K_d of SecA (no His) decreases only ~20-fold (Table 1), indicating that the dimerization of SecA Δ2-11 is more sensitive to salt concentration. At 100 mM KCl, the SecA (no His) dimer is only approximately 10-fold tighter than that of SecA Δ2-11 (Table 1). This finding is consistent with previous studies, in which SecA Δ2-11/N95 was found to exist primarily in the dimeric state in low-ionic-strength buffers (43, 44).

Alanine scanning mutagenesis demonstrates that hydrophobic amino acids near the amino terminus are critical for SecA dimerization. Concomitant mutation of 6 residues (Leu2, Ile3, Leu5, Leu6, Val9, and Phe10) to alanine (SecA-A6) completely blocks dimerization in 300 mM KCl buffer (Table 1). To further evaluate the role of these residues, several single- or double-alanine-substituted SecA variants were generated, and their dissociation constants were determined in 300 mM KCl buffer (Table 1). The L2A I3A double mutation does not substantially affect SecA dimerization, whereas the V9A F10A mutation enhances dissociation by 8-fold with respect to that of wild-type SecA. In addition, the dissociation constants of SecA mutants containing single alanine substitutions at Leu5 and Leu6 are more than three and five times that of wild-type SecA, respectively, suggesting that both residues play a role in SecA dimerization. However, no single residue appears to be critical for dimerization.

Feasibility of site-specific *in vivo* photo-cross-linking of SecA. The site-specific *in vivo* photo-cross-linking method was utilized for further determination of SecA dimer interface residues under physiological conditions. We first tested the system for SecA expression. Three residues at different positions of the 901-amino-acid SecA polypeptide, Leu6 on the amino terminus, Ser402 in the core, and Tyr820 on the carboxy terminus, were individually mutated to the amber codon, and wild-type SecA was used as a control having no amber mutation. In the absence of *p*Bpa, only fragments of SecA were produced with reduced molecular weights corresponding to truncation at the position of the amber mutation. Because the corresponding fragment from SecA L6X is so short, it is not observed on the SDS-polyacrylamide gel (Fig. 2A). Essentially no full-length SecA protein was detected for all mutants without *p*Bpa, indicating that the aminoacyl-tRNA synthetase on the plasmid pEVOL-uaaRS specifically incorporates *p*Bpa. In contrast, full-length proteins were produced for all 3 variants in the presence of *p*Bpa; however, some fragments of SecA S402X and SecA Y820X could still be detected (Fig. 2A). The expression of wild-type SecA, which lacks an internal amber codon, is similar in the absence or presence of *p*Bpa in the culture medium (Fig. 2A).

TABLE 1 Dissociation constants of SecA and its amino-terminal variants at different KCl concentrations

KCl concn (mM)	Variant[a]	K_d, μM (mean ± SD)	Source or reference
300	SecA (no His)	3.14 ± 1.81	10
	WT SecA	3.65 ± 0.19	This study
	SecA Δ2-11	ND[b]	This study
	SecA-A6	ND	This study
	SecA L2A I3A	5.99 ± 0.30	This study
	SecA V9A F10A	29.50 ± 2.51	This study
	SecA L5A	11.03 ± 2.23	This study
	SecA L6A	19.48 ± 4.84	This study
200	SecA (no His)	0.28 ± 0.13	10
	SecA Δ2-11	29.87 ± 3.72	This study
100	SecA (no His)	0.014 ± 0.009	10
	SecA Δ2-11	0.13 ± 0.03	This study

[a] WT SecA, SecA with the carboxy-terminal His tag; SecA Δ2-11, deletion of residues 2 through 11 from SecA (this is referred to as SecAΔ11 in some references [17, 28]); SecA-A6, mutant SecA L2A I3A L5A L6A V9A F10A.
[b] ND, not detectable (no dimer was detected at a concentration of up to 10 μM).

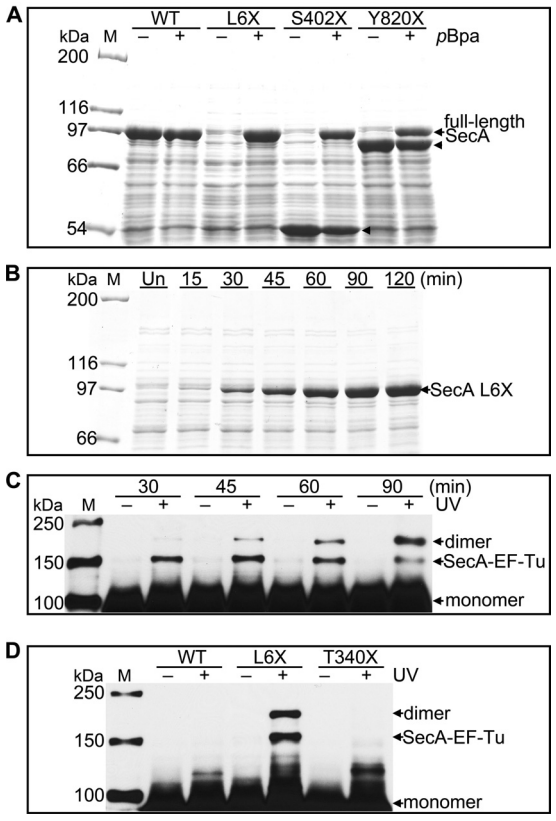

FIG 2 Expression, identification, and specificity of SecA site-specific *in vivo* photo-cross-linking. (A) SDS-PAGE analysis of the induction of wild-type SecA (WT) and SecA L6X, S402X, and Y820X in the absence (−) and in the presence (+) of *p*Bpa. Full-length SecA is produced only in the presence of *p*Bpa. The arrowheads indicate SecA fragments that likely prematurely terminated at the amber codon. Their molecular masses are consistent with the location of the amber codon used for *p*Bpa incorporation. The corresponding fragment from SecA L6X is so small that it cannot be detected by 7.5% SDS-PAGE. (B) SDS-PAGE analysis of SecA L6X expression at the indicated times after IPTG induction. Un, uninduced cells. (C) Western blot analysis of lysates from either untreated (−) or UV-irradiated (+) cells expressing SecA L6X harvested at the indicated times following induction. SecA dimer and SecA–EF-Tu, confirmed by LC-MS/MS, and monomeric SecA are indicated. (D) Comparison of the UV cross-linking pattern of SecA L6X and those of wild-type SecA (WT) and SecA T340X. Samples for panels A and B were from whole-cell lysates. Samples for panels C and D were from the soluble fraction of cell lysates. A monoclonal anti-His antibody was used for immunoblot analysis as described in Materials and Methods. Lanes M, protein molecular mass markers, with molecular masses shown on the left.

In 300 mM salt buffer, AUC revealed a dissociation constant that was ~5-fold greater than that of wild-type SecA for the single mutation L6A, suggesting that Leu6 lies on the SecA dimer interface. Hence, we developed an experimental protocol for the site-specific *in vivo* photo-cross-linking using SecA L6X. The effect of irradiation time was first evaluated with 2-h-induced SecA L6X cells (see Fig. S1 in the supplemental material). The irradiation time of 15 min yielded an optimal balance of cross-linking efficiency and Western blot signal and was therefore used in all photo-cross-linking experiments in this study. Next, the effects of induction time on SecA L6X expression and the cross-linked products were examined. Following induction at OD_{600} of ~0.6, the expression level of SecA increases with time for 120 min (Fig. 2B). However, upon UV irradiation, two cross-linked bands corresponding to ~150 and ~180 kDa are found for all time points (Fig. 2C), indicating that the identity of cross-linked products does not change with the induction time.

To further characterize the covalently cross-linked products, UV-treated SecA L6X proteins were purified via Ni-NTA chromatography and then resolved by SDS-PAGE. Two gel slices corresponding to protein molecular masses of ~150 and ~180 kDa (see Fig. S2A in the supplemental material) were subjected to in-gel trypsin digestion, and the eluted peptides were identified by LC-MS/MS. The analysis confirmed that the lower band is the adduct of SecA and the 34-kDa elongation factor Tu (EF-Tu), which has chaperone-like properties and facilitates protein folding (45). The top band contains only SecA, suggesting that it is SecA dimer. Western blot analysis shows that the SecA dimer band increases in intensity and the cross-linked SecA–EF-Tu band becomes weaker with longer expression, while the profile of SecA cross-linked products does not change; i.e., there is no evidence of nonspecific interactions (Fig. 2C). Because increasing induction time enhances the detection of cross-linked dimer bands, we subsequently harvested the SecA amber mutant cells after 1.5 to 2 h of induction (unless otherwise indicated).

To illustrate that the cross-linked bands are specific to SecA L6X, another residue, Thr340, was chosen to substitute with *p*Bpa. In contrast to SecA L6X, SecA T340X did not show the cross-linked band corresponding to SecA dimer or SecA-EF-Tu following UV irradiation. As expected, there was no detectable cross-linking of the negative control, wild-type SecA (Fig. 2D). The fidelity and efficiency of *p*Bpa incorporation and the specificity of UV cross-linking underscore the value of this approach to addressing which residues are on the SecA dimer interface.

***In vivo* evidence that residues 2 to 11 lie on the SecA dimer interface.** Because the AUC data (Table 1) indicate that mutation of residues lying at the extreme amino terminus affects SecA dimerization, we have directly assessed the contribution of this region to the dimer interface by *in vivo* photo-cross-linking. Residues 2 to 11 were separately replaced by *p*Bpa, and cells expressing these SecA variants were subjected to UV irradiation. Lysates of unirradiated cells served as negative controls. Comparable to the SecA L6X result described above, two cross-linked bands in the range of 150 to 250 kDa were detected for most variants, with the exception that SecA T7X did not show the ~150-kDa band and SecA F10X and G11X revealed a doublet at ~180 kDa (Fig. 3A).

The benzophenone group of *p*Bpa reacts with C-H bonds in close proximity; therefore, the cross-linked complexes might be the *p*Bpa-substituted SecA binding to various interaction partners, including SecA itself. To confirm that the cross-linked bands correspond to dimeric SecA, a c-myc-tagged SecA (no His) was coexpressed with each SecA variant. Western blot analysis of the lysates from cells coexpressing *p*Bpa-containing SecA and SecA-c-myc using anti-His antibody showed the same cross-linking pattern as cells expressing *p*Bpa-containing SecA alone (data not shown), indicating that cotransformation and coexpression of two SecA plasmids do not alter the cross-linking result. Western blotting using anti-c-myc antibody specifically detects the heterodimer formed between c-myc-tagged SecA and *p*Bpa-substituted SecA. Consistent with the LC-MS/MS data for SecA L6X, the expected cross-linked dimer band was also revealed with anti-c-myc antibody, while the SecA-EF-Tu band of ~150 kDa was not (Fig. 3B).

Most of the amino-terminal *p*Bpa mutants showed the same

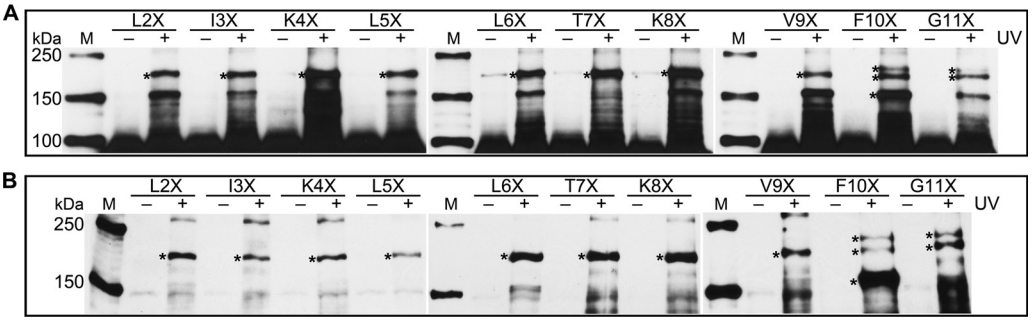

FIG 3 SecA residues 2 to 11 are involved in SecA dimerization *in vivo*. Lysates from UV-treated (+) cells expressing *p*Bpa-containing SecA (A) and *p*Bpa-containing SecA and SecA-c-myc (B) were analyzed via Western blotting and probed with antibodies specific to His tag (A) and to c-myc tag (B). The corresponding nontreated (−) cells are also shown. The amount of sample proteins loaded for panel B is 3 times higher than that for panel A. To reduce the interference from the monomer bands, the gels in panel B were run longer to allow the monomer to migrate out of the gel (same in Fig. 4B). Cross-linked SecA dimer bands are indicated with asterisks. Lanes M, protein molecular mass markers, with molecular masses shown on the left.

banding pattern as SecA L6X by Western blotting with anti-c-myc antibody (Fig. 3B). Interestingly, the major dimer band formed by SecA F10X is at ~150 kDa. The formation of several dimer bands for SecA F10X or G11X suggests that Phe10 and Gly11 are capable of interacting with multiple residues that are close in the SecA tertiary structure, and mass spectrometry confirms that these interactions are not with new binding partners. The presence of the specific cross-linked dimer bands resulting from each *p*Bpa substitution at *ec*SecA residues 2 to 11 indicates that these residues are likely on the dimer interface or in very close proximity to the associating protomer.

PBD and the IRA1 domain are involved in SecA dimerization. Five crystal SecA dimer structures (4, 23–26) show distinct dimer interfaces. To gain insight into which residues in addition to the amino terminus contribute to the *ec*SecA dimerization in solution, interface residues of these five SecA dimer structures were identified using the SPPIDER server (http://sppider.cchmc.org/), and some counterpart residues in *ec*SecA were investigated using the *in vivo* photo-cross-linking approach. Numerous residues were selected from the IRA1 domain because previous studies demonstrated that concurrent replacement of 6 residues with alanine in the region of Phe808 to Leu818 promoted SecA/N95 monomerization (13). In addition, several other residues were selected to broadly cover the SecA sequence. Beyond the amino terminus, 41 additional residues (Fig. 4A) were examined for their potential role in dimerization.

Four *p*Bpa-substituted SecA mutants with mutations in the DEAD box motor core (NBD and IRA2), SecA F68X, Y134X, T470X, and I474X, were expressed as determined by SDS-PAGE analysis of whole-cell proteins but precipitated into the pellet fraction during centrifugation, enabling detection of only a faint SecA monomer band in the soluble fraction by Western blotting with anti-His antibody (data not shown). Other variants yielded sufficient soluble SecA products for further analysis.

Most of the 41 residues examined, beyond those on the amino terminus, did not form a cross-linked band corresponding to SecA dimer (Fig. 4A; see Table S1 in the supplemental material). However, three variants, SecA F263X, Y794X, and R805X, exhibited strong and reproducible bands within the 150- to 250-kDa range. Subsequently, Phe263 of the PBD and Tyr794 and Arg805 of the IRA1 domain were confirmed to be on the SecA dimer interface using the *p*Bpa-containing SecA and SecA–c-myc coexpression system (Fig. 4B), implicating residues in the PBD and the IRA1 domain in SecA dimerization. In addition, SecA F263X and F10X produce a cross-linked dimer band with a faster electrophoretic mobility than other variants. The aberrant SDS-PAGE mobilities may result from changes in conformation dependent on the location of cross-linked residues (34), as observed in previous chemical cross-linking experiments (17, 28, 44).

Unlike the involvement of multiple consecutive amino-terminal residues on the SecA dimer interface, residues flanking Phe263, Tyr794, or Arg805 do not seem to be involved in the dimer interface, since *p*Bpa substitution of these did not lead to the formation of a SecA dimer band in our photo-cross-linking investigation (Fig. 4C). It is possible that the flanking residues do not participate in the dimer or that the benzophenone group of *p*Bpa may simply be oriented inappropriately for photo-cross-linking to occur.

Interestingly, a cross-linked band just above the monomer was detected for SecA Y794X by immunoblotting using anti-His antibody. LC-MS/MS analysis indicates that the band contains only SecA. Western blot analysis with anti-c-myc antibody did not show that band, so it is assumed to be due to intramolecular cross-linking. Similar products were formed by multiple *p*Bpa-containing SecA variants with changes in the PBD and in the IRA1 domain in response to UV irradiation (see Table S1 in the supplemental material).

The involvement of Arg805 in the SecA dimer interface depends on the presence of the amino terminus. Although SecA Δ2-11 is a monomer at 300 mM salt, it dimerizes at a 150 mM salt concentration. Thus, we investigated whether Phe263, Tyr794, and Arg805, which were found on the wild-type SecA dimer interface, also contribute to the self-association of SecA Δ2-11. Toward this end, similar cross-linking experiments were performed with SecA Δ2-11, in which these residues were individually replaced with *p*Bpa. Our experiments demonstrated that SecA Δ2-11 can dimerize in the cytoplasm, because it showed photo-cross-linking when the *p*Bpa was incorporated at Phe263 or Tyr794 (Fig. 5). Moreover, a longer induction period promoted more dimer. Surprisingly, however, SecA Δ2-11 F263X showed much stronger cross-linking than F263X in the wild-type SecA background. This may be due to higher levels of SecA Δ2-11 F263X expression (data not shown) and/or a conformational difference that permits more cross-linking of F263X in SecA Δ2-11.

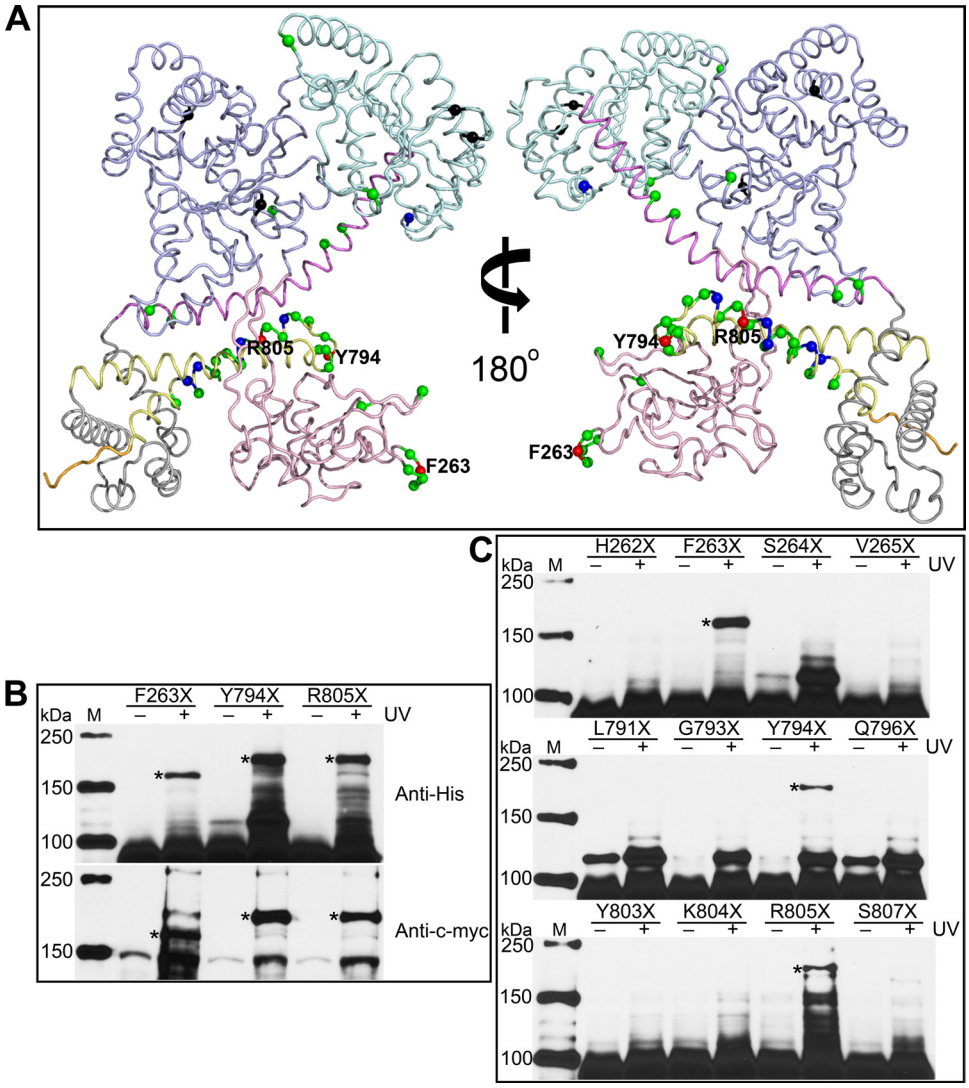

FIG 4 Phe263, Tyr794, and Arg805 are found on the SecA dimer interface. (A) Residues investigated by *in vivo* photo-cross-linking are labeled on the *ec*SecA nuclear magnetic resonance (NMR) structure (PDB ID, 2VDA) with the signal peptide masked. The structure presentation is colored according to SecA domain organization as follows: NBD, light blue; IRA2, pale cyan; PBD, light pink; SD, violet; WD, gray; IRA1, pale yellow; and CTD, orange. The colored spheres show the positions of the amber mutations. Black spheres indicate the variants expressed as insoluble proteins, and green, blue, and red spheres indicate the variants yielding no, weak, and strong cross-linked SecA dimer, respectively. Residues showing strong cross-linking signals are labeled. (B) Cross-linked SecA F263X, Y794X, and R805X dimer bands were confirmed by Western blotting with anti-His and anti-c-myc antibodies. (C) No cross-linked dimer bands form when the flanking residues of Phe263, Tyr794, or Arg805 are replaced with *p*Bpa and UV irradiated. Cross-linked dimer bands are indicated with asterisks. Lanes M, protein molecular mass markers, with molecular masses shown on the left.

In contrast, dimerization of SecA R805X was drastically affected by deletion of the amino-terminal residues, and no significant SecA Δ2-11 R805X dimer was observed, even following a 2-h induction (Fig. 5). This indicates that unlike wild-type SecA, Arg805 is not on the dimer interface of SecA Δ2-11.

DISCUSSION

SecA has the crucial role of recognizing preproteins in the cytoplasm and subsequently targeting them to SecYEG. In aqueous solution and in the cytosol, SecA undergoes a dynamic monomer-dimer equilibrium favoring its association (13). High-resolution SecA dimer crystal structures have been solved for various bacterial species (4, 23–26); however, both protomers in each structure associate through distinct dimerization interfaces (Fig. 6). These alternative interfaces may represent dimeric SecA in different states, or they may be artifacts associated with the high salt concentration used for crystallization or crystal packing effects. It is interesting that the arrangement of the SecA protomers determined in solution by cryo-electron microscopy (EM) differs from those found in any of the dimeric X-ray structures (46). It is necessary, therefore, to define the SecA dimer interface under near-native conditions.

We have examined the involvement of 51 residues (out of 901) in SecA dimerization with the *in vivo* site-specific photo-cross-linking technique, which enables characterization of protein complexes formed in intact cells (30). That the amino terminus (residues 2 to 11) was determined to be on the SecA dimer interface is in good agreement with earlier studies (17, 28) and our AUC data.

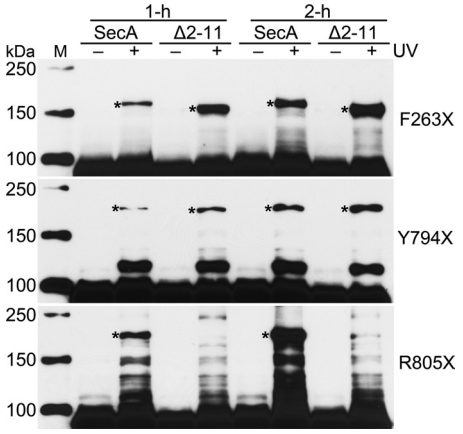

FIG 5 Comparison of cross-linking of variants F263X, Y794X, and R805X on the background of SecA and SecA Δ2-11 after 1 h and 2 h of induction. Cross-linked dimer bands are indicated with asterisks. Lane M, protein molecular mass markers, with molecular masses shown on the left.

In addition, Phe263 in the PBD and Tyr794 and Arg805 in the IRA1 domain were identified by *in vivo* UV-cross-linking to lie on the SecA dimer interface.

Mapping the residues that result in cross-linking onto the SecA dimer crystal structures indicates that no single interface contains all of the residues identified in this study (Fig. 6). Phe263 is predicted to lie on the interface in the *ec*SecA dimer crystal structure (2FSF-PBD, derived from pdb:2FSF), although the PBD was determined experimentally due to insufficient electron density making its topology less clear (4, 47). However, the positions of Tyr794 and Arg805 in this structure are inconsistent with our photo-cross-linking results because they are on the face opposite to the crystal dimer interface (Fig. 6). Interestingly, the dimer interface found in the EM structure is also incompatible with that found in the crystal structure (46). Although five dimeric SecA crystal structures exhibit distinct dimer interfaces, the counterparts of *ec*SecA Tyr794 reside on the interface in two structures (Met798 in *Mycobacterium tuberculosis* SecA [*mt*SecA] [pdb:1NL3] and Tyr743 in *bs*SecA [pdb:2IBM]) and are located near the interface in another two structures (Tyr901 in *tt*SecA [pdb:2IPC] and Tyr743 in *bs*SecA [Div_dimer]). Met754, the counterpart of *ec*SecA Arg805 in *bs*SecA, is in close proximity to the dimer interface of the Div_dimer structure. Consistent with the Div_dimer and *tt*SecA structures, our AUC and photo-cross-linking experiments indicate that the amino terminus is involved in SecA dimerization; however, these data cannot distinguish an antiparallel or parallel arrangement of dimeric SecA. Overall, our data do not fit any dimeric SecA structure completely (Fig. 6), suggesting that these interface residues may be on a SecA dimer which is distinct from any crystal structures reported to date. Considering the large size of SecA and its versatile functions in protein translocation, however, it is also possible that multiple native SecA dimeric structures exist.

Aside from the amino terminus, only a few residues were identified on the dimer interface in our experiments. Interestingly, SecA Δ2-11 forms a cross-linking profile different from that of wild-type SecA. This is consistent with the possibility that the amino terminus of one SecA protomer binds to Arg805 of the

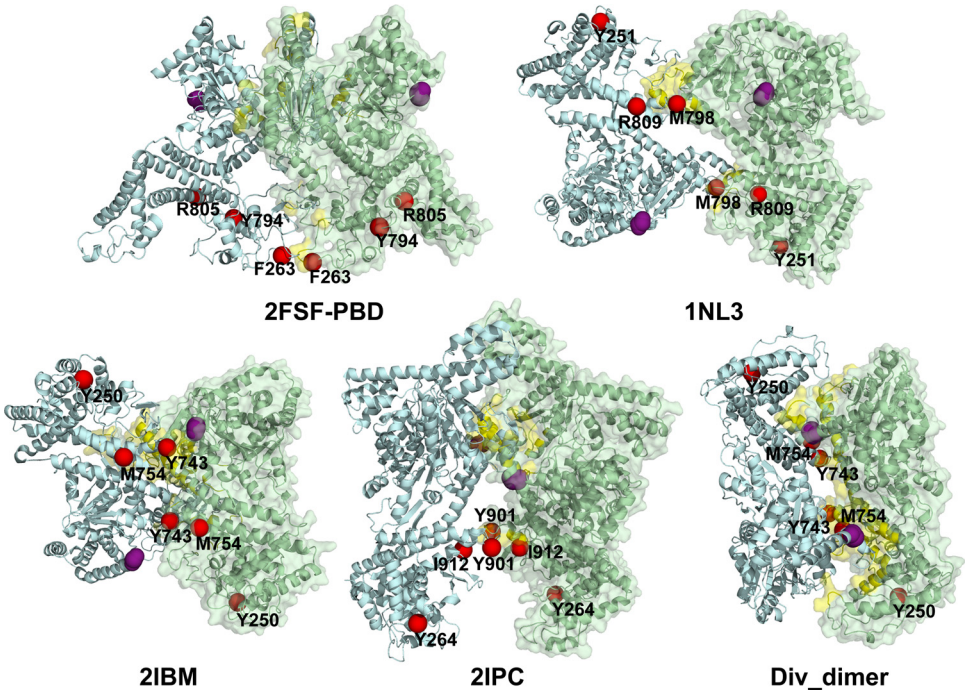

FIG 6 Positions of the *ec*SecA cross-linked residues identified here are overlaid on different SecA dimer crystal structures. One protomer (light green) is shown in cartoon and transparent surface representations and the other (gray-blue) in cartoon form only. The dimer interface revealed by the crystal structures is in yellow. Phe263, Tyr794, and Arg805 of *ec*SecA (2FSF-PBD) and their equivalent residues as defined by the sequence alignment program ClustalW on *mt*SecA (Tyr251, Met798, and Arg809 on 1NL3), *bs*SecA (Phe250, Tyr743, and Met754 on 2IBM or Div_dimer), and *tt*SecA (Tyr264, Tyr901, and Ile912 on 2IPC) are labeled and shown in red single spheres. To denote the location of the amino terminus, residue 10 in each structure is shown by four purple spheres, except in 2IBM, where it is residue 11 of chain B (gray-blue).

other. However, we cannot rule out that the conformation of SecA Δ2-11 is sufficiently different from that of wild-type SecA such that the new orientation of Arg805 indirectly hinders cross-linking. It is also unclear whether a conformational change resulting from the deletion of residues 2 to 11 strengthens the cross-linking of F263X in the context of SecA Δ2-11 relative to that in the wild type. Furthermore, another interface residue of the cytosolic SecA dimer, Tyr794, is proposed to contact and move the preprotein polypeptide chain in SecYEG-bound SecA (48), implying that SecA adopts a different conformation that does not have Tyr794 on the dimer interface during protein translocation through SecYEG. Thus, we infer that one possible function of the cytosolic SecA dimer conformation may be to prevent premature SecA translocation activity.

While we used the *in vivo* site-specific photo-cross-linking technique to map the SecA dimer interface, the cross-linking experiments also detected the SecA–EF-Tu complex with some *p*Bpa-containing variants (Fig. 3A; see Table S1 in the supplemental material). EF-Tu not only functions to bind and transport the appropriate codon-specified aminoacyl-tRNA to the aminoacyl site of the ribosome during translation but also plays a role as a chaperone facilitating protein folding (45). It is reasonable, therefore, that EF-Tu binds the expressed SecA. In addition to the association of EF-Tu with the amino terminus (Fig. 3A), we also found that SecA L815X yields a strong SecA–EF-Tu cross-linked band (see Fig. S2 in the supplemental material). Similarly, SecA Δ2-11 also cross-links EF-Tu via L815X following UV irradiation (data not shown).

While SecA Δ2-11 R805X did not form the cross-linked SecA dimer, F263X and Y794X in a SecA Δ2-11 context did, which indicates that cytosolic SecA Δ2-11 is dimeric in cells. Moreover, formaldehyde cross-linking, which links amino acids in very close proximity, also showed dimeric SecA Δ2-11/N95 *in vivo* (44). This suggests that experiments such as those evaluating specific cysteine-cysteine cross-linking that indicate that SecA Δ2-11/N95 is monomeric must be interpreted cautiously (17).

In summary, cytosolic *ec*SecA (including SecA Δ2-11) exists predominantly in a dimeric state. Our biochemical characterization of the interprotomer interaction provides information on the specific interface residues of the *ec*SecA dimer. Our data suggest that none of the crystal structures reported to date may be entirely physiological and establish the need for further investigation into SecA conformational changes during protein translocation.

ACKNOWLEDGMENTS

We thank Sarah M. Auclair for helpful discussions and Alexander C. Bertalovitz for critical reading of the manuscript. We also thank Peter G. Schultz for providing the plasmid pEVOL-uaaRS and John F. Hunt for providing the *bs*SecA dimer structure denoted by Div_dimer.

This work was supported by NIH award GM037639 to D.A.K.

REFERENCES

1. **Papanikou E, Karamanou S, Economou A.** 2007. Bacterial protein secretion through the translocase nanomachine. Nat. Rev. Microbiol. **5**:839–851.
2. **Fekkes P, de Wit JG, van der Wolk JP, Kimsey HH, Kumamoto CA, Driessen AJ.** 1998. Preprotein transfer to the *Escherichia coli* translocase requires the co-operative binding of SecB and the signal sequence to SecA. Mol. Microbiol. **29**:1179–1190.
3. **Economou A, Wickner W.** 1994. SecA promotes preprotein translocation by undergoing ATP-driven cycles of membrane insertion and deinsertion. Cell **78**:835–843.
4. **Papanikolau Y, Papadovasilaki M, Ravelli RBG, McCarthy AA, Cusack S, Economou A, Petratos K.** 2007. Structure of dimeric SecA, the *Escherichia coli* preprotein translocase motor. J. Mol. Biol. **366**:1545–1557.
5. **Cabelli RJ, Dolan KM, Qian LP, Oliver DB.** 1991. Characterization of membrane-associated and soluble states of SecA protein from wild-type and *SecA51(TS)* mutant strains of *Escherichia coli*. J. Biol. Chem. **266**: 24420–24427.
6. **Lill R, Dowhan W, Wickner W.** 1990. The ATPase activity of SecA is regulated by acidic phospholipids, SecY, and the leader and mature domains of precursor proteins. Cell **60**:271–280.
7. **Douville K, Price A, Eichler J, Economou A, Wickner W.** 1995. SecYEG and SecA are the stoichiometric components of preprotein translocase. J. Biol. Chem. **270**:20106–20111.
8. **Akita M, Shinkai A, Matsuyama S, Mizushima S.** 1991. SecA, an essential component of the secretory machinery of *Escherichia coli*, exists as homodimer. Biochem. Biophys. Res. Commun. **174**:211–216.
9. **Woodbury RL, Hardy SJS, Randall LL.** 2002. Complex behavior in solution of homodimeric SecA. Protein Sci. **11**:875–882.
10. **Wowor AJ, Yu DM, Kendall DA, Cole JL.** 2011. Energetics of SecA dimerization. J. Mol. Biol. **408**:87–98.
11. **Bu ZM, Wang LO, Kendall DA.** 2003. Nucleotide binding induces changes in the oligomeric state and conformation of Sec A in a lipid environment: a small-angle neutron-scattering study. J. Mol. Biol. **332**:23–30.
12. **Shin JY, Kim M, Ahn T.** 2006. Effects of signal peptide and adenylate on the oligomerization and membrane binding of soluble SecA. J. Biochem. Mol. Biol. **39**:319–328.
13. **Or E, Navon A, Rapoport T.** 2002. Dissociation of the dimeric SecA ATPase during protein translocation across the bacterial membrane. EMBO J. **21**:4470–4479.
14. **Benach J, Chou YT, Fak JJ, Itkin A, Nicolae DD, Smith PC, Wittrock G, Floyd DL, Golsaz CM, Gierasch LM, Hunt JF.** 2003. Phospholipid-induced monomerization and signal-peptide-induced oligomerization of SecA. J. Biol. Chem. **278**:3628–3638.
15. **Musial-Siwek M, Rusch SL, Kendall DA.** 2005. Probing the affinity of SecA for signal peptide in different environments. Biochemistry **44**: 13987–13996.
16. **Fekkes P, vander Does C, Driessen AJM.** 1997. The molecular chaperone SecB is released from the carboxy-terminus of SecA during initiation of precursor protein translocation. EMBO J. **16**:6105–6113.
17. **Or E, Boyd D, Gon P, Beckwith J, Rapoport T.** 2005. The bacterial ATPase SecA functions as a monomer in protein translocation. J. Biol. Chem. **280**:9097–9105.
18. **de Keyzer J, van der Sluis EO, Spelbrink REJ, Nijstad N, de Kruijff B, Nouwen N, van der Does C, Driessen AJM.** 2005. Covalently dimerized SecA is functional in protein translocation. J. Biol. Chem. **280**:35255–35260.
19. **Jilaveanu LB, Oliver D.** 2006. SecA dimer cross-linked at its subunit interface is functional for protein translocation. J. Bacteriol. **188**:335–338.
20. **Duong F.** 2003. Binding, activation and dissociation of the dimeric SecA ATPase at the dimeric SecYEG translocase. EMBO J. **22**:4375–4384.
21. **Kusters I, van den Bogaart G, Kedrov A, Krasnikov V, Fulyani F, Poolman B, Driessen AJM.** 2011. Quaternary structure of SecA in solution and bound to SecYEG probed at the single molecule level. Structure **19**:430–439.
22. **Zimmer J, Nam YS, Rapoport TA.** 2008. Structure of a complex of the ATPase SecA and the protein-translocation channel. Nature **455**:936–943.
23. **Hunt JF, Weinkauf S, Henry L, Fak JJ, McNicholas P, Oliver DB, Deisenhofer J.** 2002. Nucleotide control of interdomain interactions in the conformational reaction cycle of SecA. Science **297**:2018–2026.
24. **Sharma V, Arockiasamy A, Ronning DR, Savva CG, Holzenburg A, Braunstein M, Jacobs WR, Sacchettini JC.** 2003. Crystal structure of *Mycobacterium tuberculosis* SecA, a preprotein translocating ATPase. Proc. Natl. Acad. Sci. U. S. A. **100**:2243–2248.
25. **Zimmer J, Li WK, Rapoport TA.** 2006. A novel dimer interface and conformational changes revealed by an X-ray structure of *B. subtilis* SecA. J. Mol. Biol. **364**:259–265.
26. **Vassylyev DG, Mori H, Vassylyeva MN, Tsukazaki T, Kimura Y, Tahirov TH, Ito K.** 2006. Crystal structure of the translocation ATPase SecA from *Thermus thermophilus* reveals a parallel, head-to-head dimer. J. Mol. Biol. **364**:248–258.
27. **Ding H, Hunt JF, Mukerji I, Oliver D.** 2003. *Bacillus subtilis* SecA ATPase exists as an antiparallel dimer in solution. Biochemistry **42**:8729–8738.

28. **Jilaveanu LB, Zito CR, Oliver D.** 2005. Dimeric SecA is essential for protein translocation. Proc. Natl. Acad. Sci. U. S. A. **102**:7511–7516.
29. **Das S, Stivison E, Folta-Stogniew E, Oliver D.** 2008. Reexamination of the role of the amino terminus of SecA in promoting its dimerization and functional state. J. Bacteriol. **190**:7302–7307.
30. **Chin JW, Schultz PG.** 2002. *In vivo* photocrosslinking with unnatural amino acid mutagenesis. Chembiochem **3**:1135–1137.
31. **Freinkman E, Chng SS, Kahne D.** 2011. The complex that inserts lipopolysaccharide into the bacterial outer membrane forms a two-protein plug-and-barrel. Proc. Natl. Acad. Sci. U. S. A. **108**:2486–2491.
32. **Stanley AM, Carvalho P, Rapoport T.** 2011. Recognition of an ERAD-L substrate analyzed by site-specific *in vivo* photocrosslinking. FEBS Lett. **585**:1281–1286.
33. **Mohibullah N, Hahn S.** 2008. Site-specific cross-linking of TBP *in vivo* and *in vitro* reveals a direct functional interaction with the SAGA subunit Spt3. Genes Dev. **22**:2994–3006.
34. **Mori H, Ito K.** 2006. Different modes of SecY-SecA interactions revealed by site-directed in vivo photo-cross-linking. Proc. Natl. Acad. Sci. U. S. A. **103**:16159–16164.
35. **Das S, Oliver DB.** 2011. Mapping of the SecA-SecY and SecA-SecG interfaces by site-directed in vivo photocross-linking. J. Biol. Chem. **286**: 12371–12380.
36. **Farrell IS, Toroney R, Hazen JL, Mehl RA, Chin JW.** 2005. Photo-cross-linking interacting proteins with a genetically encoded benzophenone. Nat. Methods **2**:377–384.
37. **Schmidt MO, Brosh RM, Oliver DB.** 2001. *Escherichia coli* SecA helicase activity is not required *in vivo* for efficient protein translocation or autogenous regulation. J. Biol. Chem. **276**:37076–37085.
38. **Young TS, Ahmad I, Yin JA, Schultz PG.** 2010. An enhanced system for unnatural amino acid mutagenesis in *E. coli*. J. Mol. Biol. **395**:361–374.
39. **Laue TM, Shah BD, Ridgeway TM, Pelletier SL.** 1992. Computer-aided interpretation of analytical sedimentation data for proteins, p 90–125. *In* Harding SE, Rowe AJ, Horton JC (ed), Analytical ultracentrifugation in biochemistry and polymer science. Royal Society of Chemistry, Cambridge, United Kingdom.
40. **Stafford WF, Sherwood PJ.** 2004. Analysis of heterologous interacting systems by sedimentation velocity: curve fitting algorithms for estimation of sedimentation coefficients, equilibrium and kinetic constants. Biophys. Chem. **108**:231–243.
41. **Shevchenko A, Tomas H, Havlis J, Olsen JV, Mann M.** 2006. In-gel digestion for mass spectrometric characterization of proteins and proteomes. Nat. Protoc. **1**:2856–2860.
42. **Porollo A, Meller J.** 2007. Prediction-based fingerprints of protein-protein interactions. Proteins **66**:630–645.
43. **Gold VAM, Robson A, Clarke AR, Collinson I.** 2007. Allosteric regulation of SecA—magnesium-mediated control of conformation and activity. J. Biol. Chem. **282**:17424–17432.
44. **Wang HY, Na B, Yang H, Tai PC.** 2008. Additional *in vitro* and *in vivo* evidence for SecA functioning as dimers in the membrane: dissociation into monomers is not essential for protein translocation in *Escherichia coli*. J. Bacteriol. **190**:1413–1418.
45. **Caldas TD, El Yaagoubi A, Richarme G.** 1998. Chaperone properties of bacterial elongation factor EF-Tu. J. Biol. Chem. **273**:11478–11482.
46. **Chen Y, Pan X, Tang Y, Quan S, Tai PC, Sui SF.** 2008. Full-length *Escherichia coli* SecA dimerizes in a closed conformation in solution as determined by cryo-electron microscopy. J. Biol. Chem. **283**:28783–28787.
47. **Gelis I, Bonvin AM, Keramisanou D, Koukaki M, Gouridis G, Karamanou S, Economou A, Kalodimos CG.** 2007. Structural basis for signal-sequence recognition by the translocase motor SecA as determined by NMR. Cell **131**:756–769.
48. **Erlandson KJ, Miller SBM, Nam Y, Osborne AR, Zimmer J, Rapoport TA.** 2008. A role for the two-helix finger of the SecA ATPase in protein translocation. Nature **455**:984–987.